

Adsorption-Semiconductor Sensor Based on Nanosized SnO₂ for Early Warning of Indoor Fires

Nelli Maksymovych, Ludmila Oleksenko and George Fedorenko

Abstract

The paper is devoted for a solution of indoors fires prevention at early stage by determination of H₂ (fire precursor gas) in air using a semiconductor sensor. A material based on Pt-containing nanosized tin dioxide with an average particle size of 10–11 nm obtained via a sol–gel method was created for a gas sensitive layer of the sensor. The developed sensor has high sensitivity to H₂ micro concentration, a wide range of its detectable content in air, selectivity of H₂ measuring in the presence of CO and CH₄, good dynamic properties. The combination of these properties is very important for prevention of inflammations on their early stages before the open fires appearance. Economic benefit of the proposed sensor is due to a lower cost and higher reliability of the fire situation detection.

Keywords: early fire detection, sensor, semiconductor, nanomaterial, tin dioxide, platinum

1. Introduction

Fires detection is an urgent task today, since every year, a large number of the fires occurs all over the world, leading to human casualties and economic losses. It can be seen from the **Figure 1** that fires take place in all countries of the world regardless gross domestic product values and level of technology development.

These fires appear from various sources of ignition (structure fires, vehicles, forests, grass, rubbish) as shown in **Figure 2**.

The fires that occur in premises (the structure fires) are of particular importance among all fires, since they lead to human casualties (**Figure 3**). Besides, these fires lead to significant and often irreparable economic losses.

The decrease in the number of the fires and their consequences are determined mainly by the presence of special warning means, the so-called fire-alarm-systems. When the fire-alarm-system is creating the main responsibility lies on the choice of reliable detectors appropriate for providing a timely alert of inflammation. Modern fire detectors can be conventionally divided into the following groups: **heat detectors** registering a temperature increase while the inflammation is present; **smoke detectors** operating due to ionization or photoelectric effects; **flame detectors** based

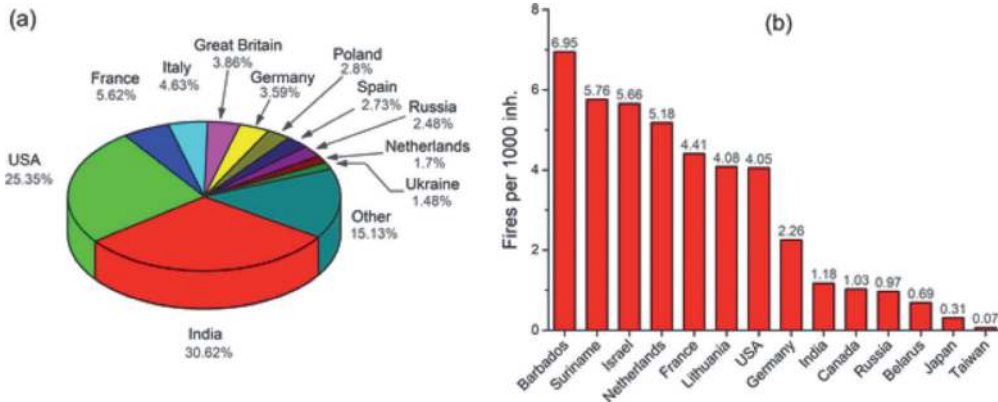


Figure 1. Average annual fires distribution in percent within 65 countries (a) and average annual number of fires per 1000 inhabitants (b) in 2014–2018 years [1].

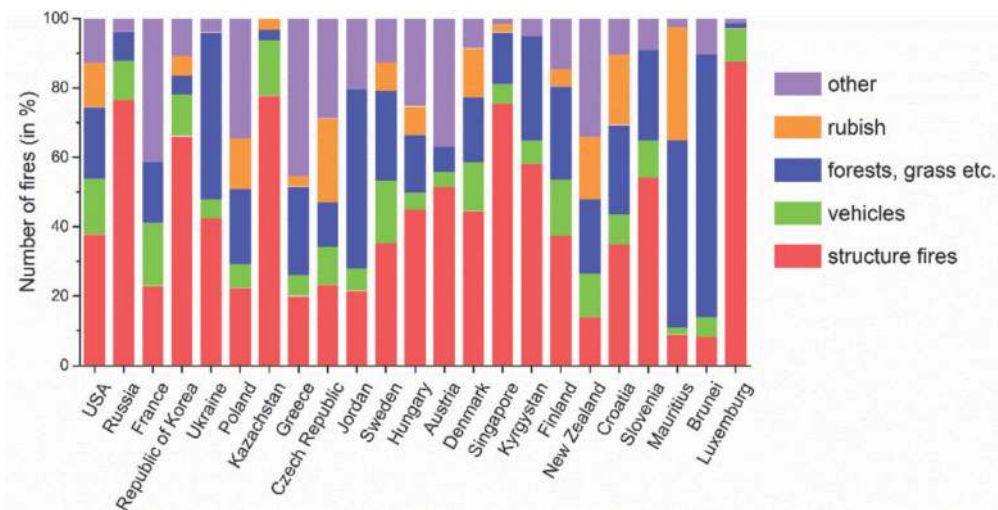


Figure 2. Distribution of fires by types in the countries of the World in 2018 [1].

on the use of ultraviolet or infrared irradiation and **gas detectors** registering changes in gas composition of surrounded air as a result of the inflammation [2, 3].

Among them the heat detectors and flame detectors are not capable of early registration of the fire, because they response on increasing temperature caused by a hot air flow, or by electromagnetic irradiation in various ranges of a spectrum attributed to burning process. All those physical phenomena are observed when the fire is already spread around several square meters. In the contrast to the heat detectors, smoke detectors give a fire-alert before the open flame will be present. But the walls of a smoke detector chamber become dusty with time that can cause false fire-alert and heat detectors that register an increase temperature of air in rooms are rather crude and cannot detect the occurrence of the fire at the smoldering stage. **Figure 4** shows some types of the fire-alarm systems with the above mentioned detectors.

Nowadays the above mentioned kinds of the fire detectors are widely eliminated by more universal systems based on analysis of a chemical composition of air which changes dramatically when processes of thermal decomposition of the overheated inflammable materials take place [4–6]. The type of gases produced at the initial



Figure 3. Average annual number of fire death and injuries per 100 fires (in 2014–2018 years) [1].



Figure 4. Fire alarm systems based on different types of detectors: a – heat-type IP 105-1 D; b – smoke-type DUR-40 Ex; c – flame-type IP 330/1-20; d – gas type IP 435-1.

stage of combustion are determined by the composition of materials involved in this process, however, in the most cases, the main components of the appeared gases (fire precursors) can be distinguished. In particular, in the work [7] it has been experimentally established that the first gas component released during decay (pyrolysis) of wood, textiles, synthetic materials covering metal wires (telephone and electric) is hydrogen and its concentration at the early stage of ignition reaches 20–25 ppm. It is important, that appearance of CO and CH₄, during the ignition, for example,

of wood, polyethylene (PE), polyurethane (PUR) and mixtures of these materials (mixed crib) is observed only at a later stage, as can be seen from the data presented in **Table 1**.

In this case, as established experimentally in study of the combustion of various objects commonly used in domestic premises (**Table 2**), the appearance of CO for some of them was not observed at all (for sponge and food), or CO appeared in air only at significant burning time (for wood). The appearance of smoke, in the amount required for responses of the smoke detectors, is observed only at a significant heating time of burning objects (except of the sponge). But the production of hydrogen was always observed for all studied materials immediately after beginning of the heat (except for the roll), and a signal values for the gas sensor reached a large value, especially for the wood and sponge (the latter used as an example of organic matter because a lot of household items in premises consist it (wallpaper, furniture, dishes, etc.)).

Thus, the detection of fire at the early stage of ignition is possible by measuring the concentration of hydrogen, which is almost always can be detected in air of the room where the fire occurs, and which appears the first of the gases - precursors of

Gas	Wood		PUR		PVC		Mixed crib	
Hydrogen	Time (min)	Signal (mV)	Time (min)	Signal (mV)	Time (min)	Signal (mV)	Time (min)	Signal (mV)
	0–10	0–15	0–5	0	0–5	<5	0–10	<5
	10–20	15–37	5–10	0–10	5–10	5–10	10–20	5–10
	20–45	37–40	10–20	10–30	10–80	10–25	20–40	10–15
	45–50	30–40	20–70	30–35			40–60	15–20
						60–80	20–30	
						80–100	30	
Carbon monoxide	Time (min)	Conc. (ppm)	Time (min)	Conc. (ppm)	Time (min)	Conc. (ppm)	Time (min)	Conc. (ppm)
	0–10	0–5	0–5	0	0–80	<2	0–70	<2
	10–20	5–12	5–10	0–12			70–100	2–5
	20–30	12–20	10–15	12–7				
	30–40	20–25	15–65	7				
40–50	25–27	65–70	<7					
Smoke detectors	Time (min)	Detector alarm	Time (min)	Detector alarm	Time (min)	Detector alarm	Time (min)	Detector alarm
	5	1st detector	No alarms		No alarms		No alarms	
	10	2nd detector						

¹CO concentration was measured by Fourier transformed infrared spectroscopy, H₂ concentration was measured using a gas sensor based on a metal/solid electrolyte/insulator. Presence of smoke was determined by a commercial smoke detector [7].

Table 1. Occurrence of hydrogen, carbon monoxide and smoke in air with the pyrolysis time of different materials: Wood, polyethylene (PE), polyurethane (PUR) and mixtures of these materials (mixed crib).

Gas	Armchair		Roll		Sponge		Food	
Hydrogen	Time (min)	Signal (mV)	Time (min)	Signal (mV)	Time (min)	Signal (mV)	Time (min)	Signal (mV)
	0–10	<10	0–40	<5	0–3	0–50	0–10	<5
	10–20	10–30	40–60	5–10	3–10	50–60	10–20	5–20
	20–30	30–40	60–80	10–70	10–25	60–65	20–30	20–30
	30–40	40–60	80–100	70	25–40	50–65	30–40	30
	40–45	60–70						
	45–50	50–60						
Carbon monoxide	Time (min)	Conc. (ppm)	Time (min)	Conc. (ppm)	Time (min)	Conc. (ppm)	Time (min)	Conc. (ppm)
	0–5	0	0–50	0	0–40	<5	0–40	<5
	5–10	<5	50–60	<5				
	10–20	5–10	60–70	5–40				
	20–30	10–15	70–100	40–50				
	30–40	15–25						
	40–50	25–30						
Smoke detectors	Time (min)	Detector alarm	Time (min)	Detector alarm	Time (min)	Detector alarm	Time (min)	Detector alarm
	20	1st detector	60	1st detector	2	1st detector	24	1st detector
	40	2nd detector	65	2nd detector	4	2nd detector	2nd detector – no alarm	

^aCO concentration was measured by Fourier transformed infrared spectroscopy, H₂ concentration was measured using a gas sensor based on a metal/solid electrolyte/insulator. Presence of smoke was determined by a commercial smoke detector [7].

Table 2. Occurrence of hydrogen, carbon monoxide and smoke in air with the time of pyrolysis of various household items: Armchair, roll, sponge, food with the time of their heating.^a

the fire. At the early stage of the ignition it is still possible to assume adequate action and take control over the situation. For example, in a case of electricity wires being overheated it is not late to switch them off automatically, thus preventing the fire at the beginning.

Although the appearance of certain gases in air during the ignition of materials is separated in time, but reliable detection of the fire based on the hydrogen released at the first stage of combustion is possible only with sufficient selectivity of the sensor to hydrogen. But the sensors are known to do not possess good selectivity [8, 9].

That is why, for the early prevention of the fire, the gas sensors are included in complex systems, for example, in the MAGIC.SENS Automatic LSN Fire Detector (Bosch), that provides multipurpose detection of the fire-hazard using a joint action of optical, thermal and chemical sensors. Undoubtedly, a signal of such kind of the multiple-purpose detectors considerably increases veracity of the fire diagnostics, while the separate use of the detectors of this system do not provide effective diagnostics of the fire situation. Indeed, using only a thermal detector will not allow determining the onset of smoldering materials, in the presence of dust the false fire alerts

of an optical detector are possible, and using only a gas sensor in the system will not provide diagnostics due to its low selectivity to gases emitted during the fire.

At the same time, possessing, in general, insufficient selectivity, the semiconductor gas sensors have a number of other capabilities (high sensitivities to gases, good response time, a wide range of gas detection, an ability to operate in a significant range of the ambient temperatures ($-45 \div +45^{\circ}\text{C}$), low mass and dimensions), which make them promising for creation of devices and systems capable to provide reliable diagnostics of the onset of the fires.

The design of the semiconductor sensor created at the Department of Chemistry of the Taras Shevchenko National University of Kyiv is present in **Figure 5**.

The sensor consists of a ceramic plate with platinum heater on one side and Pt contacts on the opposite side of the plate (**Figure 5a**). These contacts intended to measure the current flowing through a gas sensitive layer deposited between them (**Figure 5b**). The gas sensitive layer is made of semiconductor material, whole sensor has a very small size ($2 \times 2 \times 0,5$ mm, **Figure 5c**).

A principle of the semiconductor sensor operation is based on a change in its conductivity in the presence of the analyzed gas in air. **Figure 6** shows schematically the sensor sensitivity mechanism from the standpoint of the band theory of semiconductors [11].

In the absence of the analyzed gas in air (**Figure 6A**), chemisorption of oxygen occurs on the sensor surface with localization of electrons from the semiconductor conduction band on the oxygen atoms [12, 13]. Reduction of the electrons number in the conduction band of the semiconductor leads to decrease in its electrical conductivity. In the presence of the analyzed gas R (**Figure 6B**), its molecules interact with the active chemisorbed oxygen. The electrons, previously localized on the chemisorbed oxygen, return to the conduction band of the semiconductor and increase its conductivity. This increase will be the greater if the concentration of gas R will be higher. This is the basis for the use of semiconductor materials in the sensors for determination of the concentration of the analyzed gas R. Finally, **Figure 6C** shows a role of the catalytic additive (Me), that increases a rate of catalytic oxidation reaction by the chemisorbed oxygen through activation of the R molecules, that leads to an even larger number of electrons returned to the conduction band - the sensor

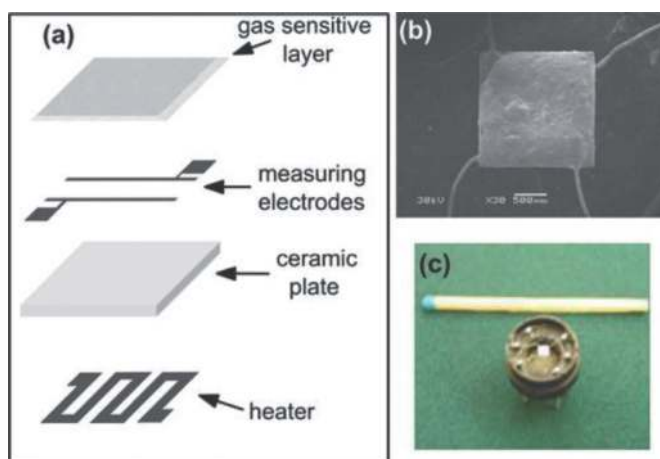


Figure 5. Design of the semiconductor gas sensor: a – schematic illustration of the main elements of the semiconductor gas sensor; b – view of a ceramic sensor plate with a sensitive layer; c – SEM image of the sensor in its measurement chamber [10].

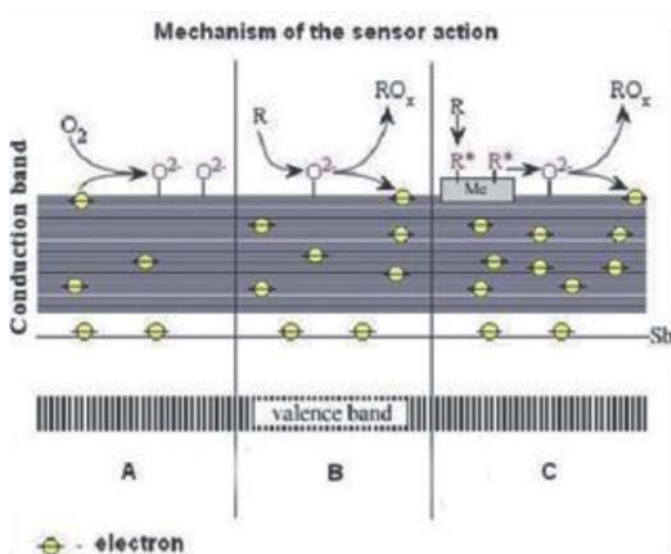


Figure 6. Schematic illustration of the action mechanism of the semiconductor sensors: A – Sensor material in absence of analyzed gas (R); B – Sensor material exposed to the analyzed gas; C – Doped by catalytic additive me sensor material exposed to the analyzed gas.

sensitivity to the analyzed gas becomes greater [14, 15]. This simple scheme shows a reason for the low selectivity of the sensor: at a given sensor temperature, molecules of many gases can overcome the energy barrier of the oxidation reaction [16] thereby increase the conductivity of the sensor.

Several devices were created at the University using semiconductor sensors (Figure 7). In particular, with combination of the sensor and previous chromatographic separation of the air sample, it was possible to ensure absolute selectivity of CH₄, C₂H₆ and C₃H₈ measurements that was applied in a developed portable chromatograph intended to determine natural gas leaks from pipelines without digging the soil (Figure 7b).

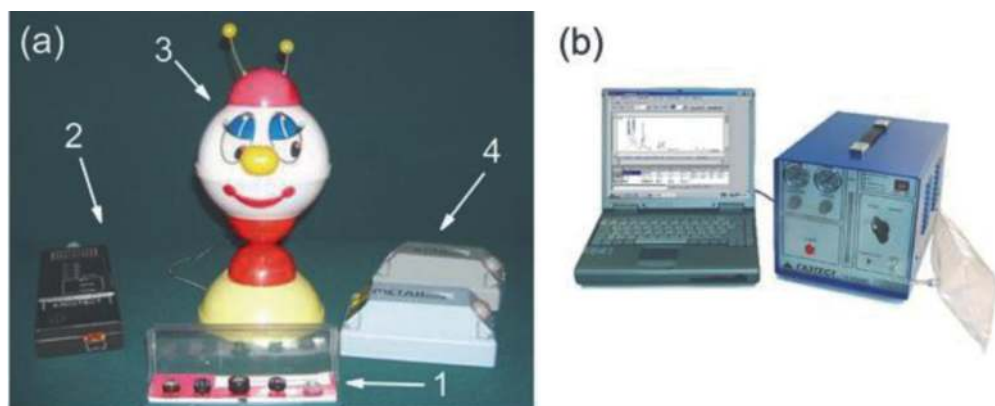


Figure 7. Examples of developed devices based on semiconductor sensors created at the Taras Shevchenko National University of Kyiv: Semiconductor sensors (1, a), a device intended to determine alcohol in exhaled air (2,a), a domestic device in the form of a doll intended to determine presence of methane in air of kitchen (3,a), a device intended to determine concentrations of methane in air purposed for vehicles (4, a) a portable chromatograph intended to determine natural gas leaks from pipelines without digging soil (b) (Project #840 of Science and Technology Center in Ukraine).

It should be noted that although the sensors have low selectivity, changes in the chemical compositions of the gas sensitive layers, their morphology and temperature can affect the rates of gases oxidation on the semiconductor surfaces and, thus, regulate the selectivity of measurement. These approaches allow to avoid the use of the sensors in conditions of the chromatography, that neutralize attractive possibilities of using the low-power sensors in the corresponding miniature portable devices or as sensors of stationary automated systems for monitoring indoor air.

In our work, tin dioxide, an n-type semiconductor, was chosen as a basis of the sensitive layer of the sensor [17]. Tin dioxide exhibits high chemical and thermal inertness, that is necessary to ensure a long-term stable operation of the sensor in the practice [12]. In order to increase the sensor response, the material of the gas sensitive layer based on tin dioxide was obtained in a nanoscale state [13, 14, 17]. This should ensure that the processes occurring on the gas sensitive surface of the sensor have a predominant effect on its volumetric characteristics, in particular, on the values of its electrical conductivities [18]. Taking into account the mechanism of the sensor response formation [12–15, 17], a catalytically active additive was introduced into its gas sensitive layer, that allows to accelerate the process of the oxidation of hydrogen by the oxygen chemisorbed on the sensor surface. One of such catalytic additive may be platinum, which has an extremely high activity in the oxidation reaction of H₂ [19] and it is much higher than in the oxidation reaction of CO and CH₄.

The aim of our work is to develop a fast semiconductor gas sensor based on nano-sized SnO₂ possesses very high sensitivity to H₂ microconcentration and low sensitivities to CO and CH₄ purposed for systems of fires detection at early stage.

2. Materials and methods of investigation

The initial substances for synthesis of the material of the sensitive layer were SnCl₄ × 5H₂O, ethanediol-1,2, and H₂PtCl₆.

In order to synthesize SnO₂ 1.5 g of SnCl₄·5H₂O were added to 15 ml of ethanediol-1,2 under sintering. The mixture was heated to 353 K until the salts were completely dissolved. The resulting solution was transferred to a ceramic dish and then was kept at 393 K C in a sand bath until approximately 80% of the solvent (by a volume) was evaporated. A resulting dark brown viscous gel was aged in air at a room temperature for 30 minutes, then kept in an oven at 423 K for two days. The obtained brown xerogel was subjected to heat treatment with limited air access in a temperature range from 298 K to 873 K according to a special sintering program in a programmable oven “GERO” (Germany). The temperature mode of the program is shown in **Figure 8**. A light yellow nanosized SnO₂ was obtained as a result of the treatment. Semiconductor sensors were created by applying a paste, consisted of the obtained nanosized SnO₂ and an aqueous solution of carboxymethylcellulose, between the measuring electrodes of the ceramic plates of the sensors. Then the plates with applied paste were dried at 363 K impregnated with a solution of hexachloroplatinic acid (5,3x10⁻²M) and heated up to 892 K.

Study of the obtained nanomaterials by transmission electron microscopy (TEM) was performed on an electron microscope Selmi TEM - 125 K with an accelerating voltage of 100 kV and by X-ray diffraction analysis (XRD) diffractometer on a Bruker D8 Advance diffractometer with CuK α radiation.

Study of the sensor characteristics was performed in a special electric stand (**Figure 9**).

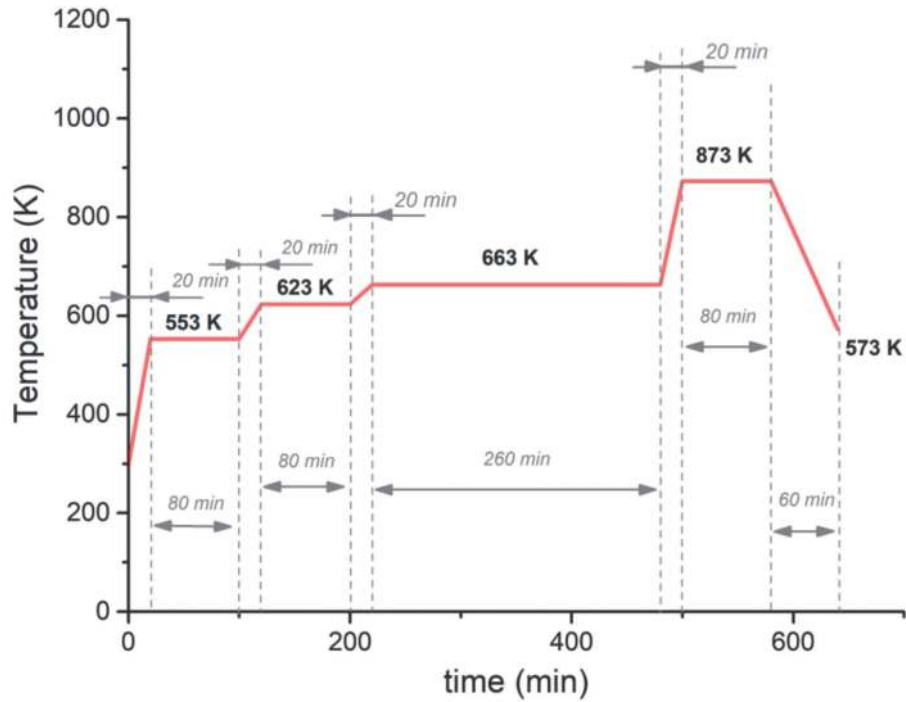


Figure 8.
 A special thermal program for xerogel sintering.

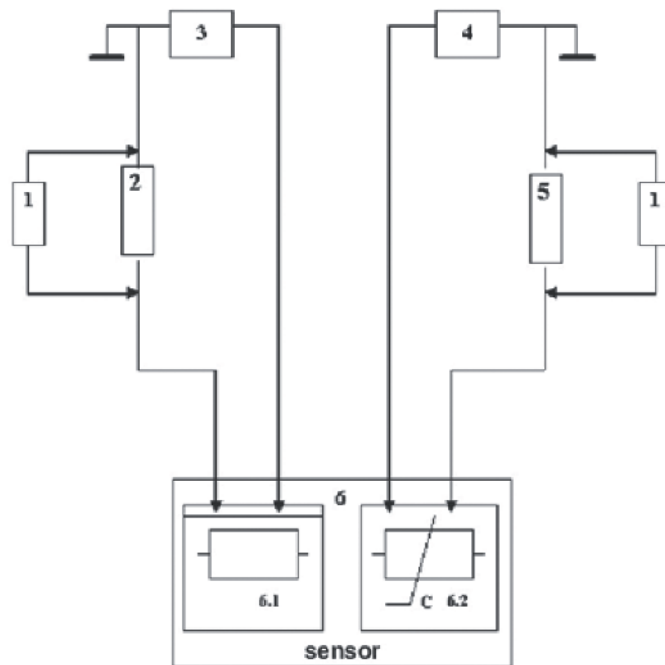


Figure 9.
 Electrical diagram of the stand intended to determine the parameters of the sensors: A1 - power supply of the sensor heater; 1 - voltmeter or recording devices; 2 - a resistor for current registration through the sensor heater; 3 - power supply of the heater of the sensor; 4 - power supply of the sensitive layer of the sensor; 5 - a load resistor; 6 - a semiconductor sensor (6.1 - a heater; 6.2 - a sensitive layer).

The electrical resistance of the sensor (R_s) was calculated according to the Ohm's law for series connection of conductors:

$$R_s = R_l (U - U_l) / U_l \quad (1)$$

where U - voltage of the power supply of the sensitive layer; U_l is voltage drop on the load resistor; R_l is a value of the resistance of the load resistor.

The following notations were used to evaluate the properties of the sensors: R_o is the electrical resistance of the sensor in pure air, R_g is the electrical resistance of the sensor in the presence of an analyzed gas R . A ratio of the sensor electrical resistance in pure air to the electrical resistance in the analyzed gas – air mixture (R_o/R_g) was considered as a response of the sensor to this gas.

Before measuring the characteristics of the sensors, they were purged by a gas mixture with a hydrogen concentration of 935 ppm every 1 hour for three days at a temperature of the gas sensitive layer 675 K in order to stabilize sensors resistances.

Sensor response time ($t_{0,9}$) was defined as the time to reach 90% of the constant value of the sensor response in the presence of the analyzed mixture, the sensor relaxation time (τ_r) was defined as the time to reach the sensor 10% of the sensor response when replacing analyzed gas mixture by pure air.

The investigated gas mixtures were prepared in pressure cylinders and certified at Ukrmetrteststandard.

3. Results and discussion

Figure 10 shows a schematic illustration of nanosized tin dioxide synthesis via sol-gel method, that allows to achieve high chemical homogeneity of products, particle size control and morphology of the material at different stages of synthesis by changing temperature, reaction time, nature of solvents, chemical composition and reagent concentrations [20–22].

In contrast to the most common variant of the sol-gel method, where water is used as a solvent and the final hydroxide or oxide is obtained by alkaline or acid hydrolysis [21, 22], the non-aqueous variant of the “classical” method has a number of advantages over the method. Ethylene glycol is used as a solvent that at the same time acts as a hydrolytic agent, reacting chemically with tin (IV) chloride to form HCl

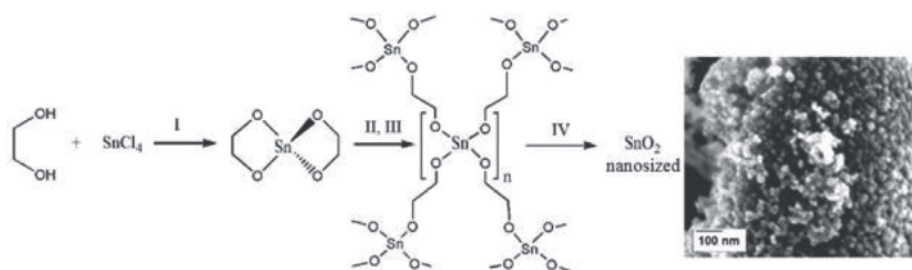


Figure 10. Scheme of the nanosized SnO_2 synthesis by a sol-gel method: I –dissolving of SnCl_4 in ethylene glycol at 353 K II and III - evaporation of the obtained solution on a sand bath with consequent drying it in an oven; IV - heat treatment up to 873 K. SEM image of the synthesized SnO_2 is shown in insert.

and corresponding tin (IV) glycolate (**Figure 10**, stage I). Then, as the temperature rises, the glycolate is polymerized to form a three-dimensional grid (**Figure 10**, stages II, III), where ethylene glycol molecules act as bridges between tin atoms. Thus, ethylene glycol performs a structure-forming function. In addition, ethylene glycol also performs an important function of preventing agglomeration of particles during the heat treatment of the xerogel in an oven, as bimethylene linkers are quite stable and completely burn out of the material only at a temperature about 773 K [23]. Thus, in initial stages of the process, when the temperature rises and the oxide particles are just beginning to form, ethylene glycol molecules partially prevent the process of the nanoparticle aggregation.

According to TEM observation, the synthesized nano-SnO₂ material consists of spherical particles with an average size 10–11 nm (**Figure 11a**).

According to X-ray diffraction analysis, the obtained tin dioxide has a cassiterite structure (ICDD PDF - 2 version 2.0602 (2006), card 00. 00–041-1445), and no other phases were found in the obtained material (**Figure 12**).

Calculation of the particle size according to the Scherrer equation (XRD size) [24] has shown that the size of the coherent scattering region for the obtained material is 6.7 nm. The significant difference between the particle size according to TEM data and those calculated according to the Scherrer equation can be explained by existence of an amorphous surface layer or the presence of defects in the tin dioxide crystal lattice on the surfaces of nanoparticles [25, 26]. This may be due to the formation of the crystal structure of tin dioxide in the presence of the organic matrix, that has not yet fully oxidized in the conditions of the heat treatment [23].

It was established that the thermal formation of the semiconductor materials of the gas-sensitive layer (at temperatures up to 620°C) leads to the aggregation of SnO₂ particles. This effect can explain increase in particle size for the sensor materials in comparison with the initial SnO₂. For example, average TEM size of the semiconductor particles for the undoped sensor materials is 19–20 nm while average TEM size of the initial SnO₂ is equal to 10–11 nm [27]. No changes in the phase composition of the gas-sensitive layer were detected by the X-ray diffraction analysis, and the average particle size of tin dioxide material, calculated by the Scherrer equation, was 20.1 nm [27]. This correspondence between the values of the average particle size obtained by the different methods (TEM and X-ray diffraction) may indicate that additional high-temperature treatment in the formation of the gas sensitive materials reduces significantly a number of defects in the crystal lattice of tin dioxide.

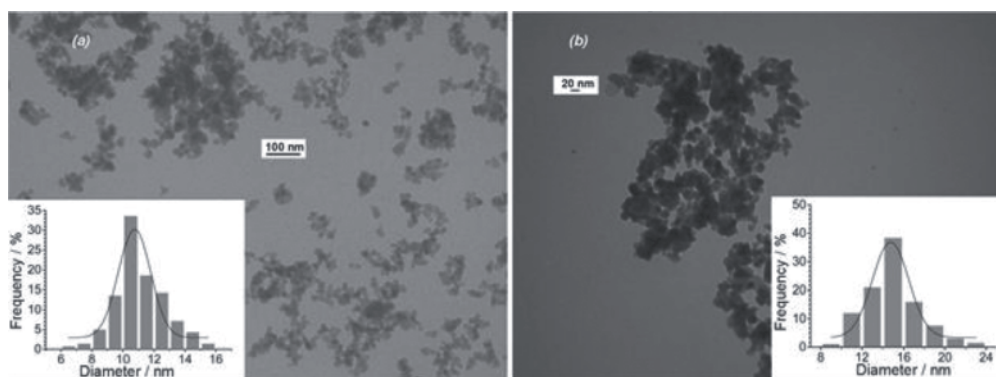


Figure 11. TEM images of the initial tin dioxide (a) and platinum-containing sensor material obtained by impregnation with 5.3·10⁻² M solution of H₂[PtCl]₆ (b).

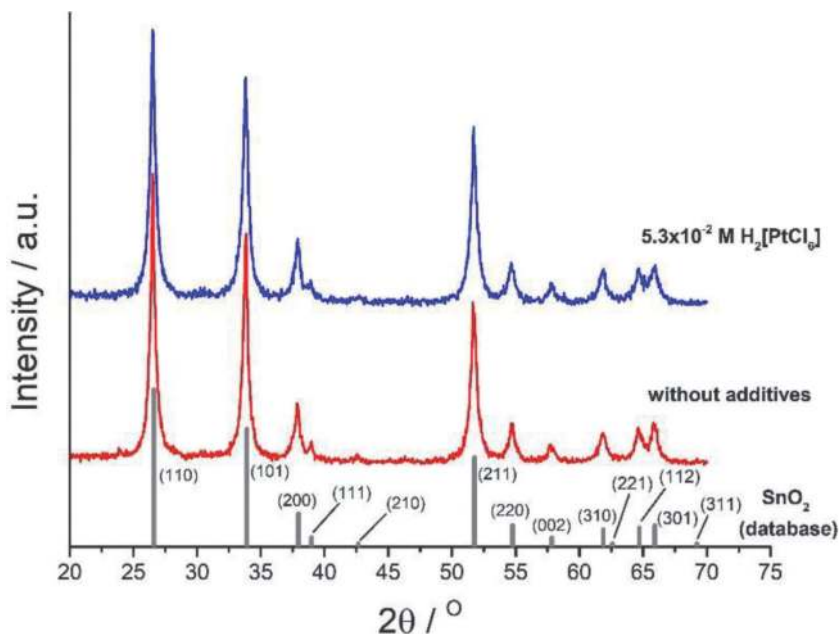


Figure 12. X-ray diffraction of the sensor material without additives and platinum-containing sensor material (obtained by impregnation with $5.3 \cdot 10^{-2}$ M solution of $H_2[PtCl_6]$).

Analysis of TEM images of the platinum-containing gas sensitive materials (**Figure 11b**) revealed that addition of platinum reduces significantly the average particle size of the tin dioxide material (from 19 to 20 nm to 14–15 nm). The particle sizes calculated by TEM and X-ray diffraction methods are the same, that indicates to good crystallization of tin dioxide in the platinum-containing sensor material.

Figure 13a shows the dependence of the sensor response to hydrogen (22 ppm) on the temperature of the sensor. As it can be seen, this dependence has an extreme character with a maximum response of the sensor at the temperature 595 K, that may be caused by oxygen adsorption–desorption processes on the surface of the semiconductor layer.

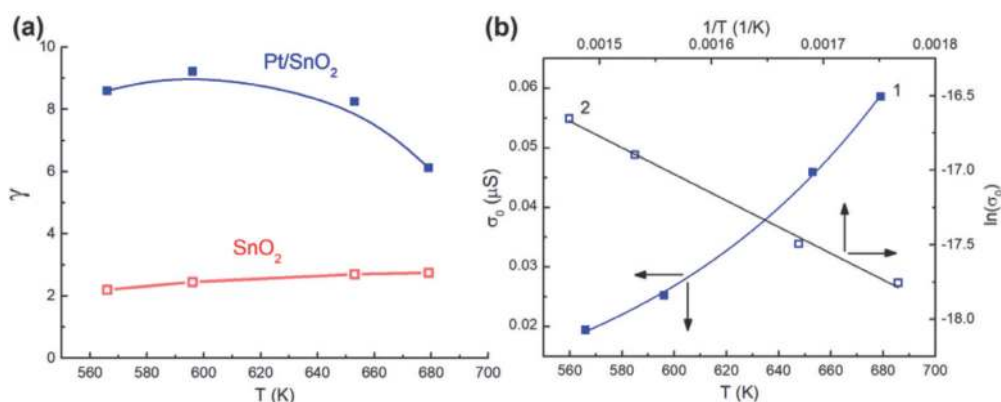


Figure 13. The dependence of the sensor response to 22 ppm of hydrogen on the temperature of the sensor (a) and (b) - the dependence of the electrical conductivity in air (σ_0) on its temperature in the coordinates σ_0 from T (1) and $\ln(\sigma_0)$ from $1/T$ (2) for the sensor based on Pt/SnO₂.

To explain the obtained data, it should be taken into account that in the presence of hydrogen the charged forms of oxygen formed by the oxygen chemisorption on the surface of the gas sensitive layer are able to oxidize H₂ molecules activated on platinum particles that leads to return of the electrons in the conduction band of the semiconductor and increases its conductivity. Naturally, if the rate of the oxidation of hydrogen is higher and, as a consequence, the greater is amount of the chemisorbed oxygen on the surface of the semiconductor is involved in oxidation of H₂ molecules, the response of the sensor will be higher. It can be assumed that increase in the operating temperature of the sensor from 565 to 595 K leads to an increase in the amount of the oxygen chemisorbed on the surface of the gas sensitive layer and consequently to an increase in the response of the sensor from 8.6 to 9.2, respectively. A further decrease in the response of the sensor with increasing the operating temperature may be due to the dominance of the desorption of the chemisorbed oxygen from the surface of the semiconductor. At the same time, this assumption is contradicted by the experimental data shown in **Figure 13b**. These data show a monotonic increase in the conductivity of the sensor under conditions of the increasing temperature, which cannot explain the initial stage of increasing the response of the sensor to hydrogen (**Figure 13a**) by increasing the amount of the chemisorbed oxygen. To understand this discrepancy, it is necessary to consider the main factors that determine it.

As can be seen from **Figure 13b**, an increase in the temperature of the sensor leads to an increase in its conductivity according to the exponential law (**Figure 13b**, curve 1), that is characteristic of semiconductors [28]. This dependence can be linearized in the coordinates $\ln(\sigma) - 1/T$, that allows to calculate the activation energy of conductivity. It was found that a value of the activation energy in the operating temperature range of the sensor 565–680 K is 0.65 eV. This value is characteristic of the interparticles barrier between the grains of tin dioxide [29] indicating a slight effect of the oxygen chemisorbed at the interface between the particles of platinum and tin dioxide on the value of activation energy of the conductivity of Pt/SnO₂. That is why a change in the conductivity of the sensor from the temperature (**Figure 13b**, curve 1) does not reflect the effect of the chemisorbed oxygen on the conductivity of the sensor, which is usually observed for sensor systems [30]. Since an increase in the temperature of the sensor leads to an increase in its conductivity that is a result of an increase in the number of charge carriers (electrons) capable to overcome the interparticles barrier, an increase in the temperature leads to a decrease in the width of the space charge region (SCR). It is known that the width of the SCR is one of the factors that can directly affect the response of the sensor [12–14]. Likely, for the sensors based on nanosized Pt/SnO₂ material, an increase in the temperature leads to a significant decrease in the width of the SCR. As a result, the surface processes, such as the involving of the chemisorbed oxygen on the SnO₂ surface in the oxidation of H₂ molecules, are masked by their own high conductivity of the semiconductor and therefore the processes of the oxygen chemisorption are not reflected in the change in the conductivity of the sensor with increasing the temperature (**Figure 13b**, curve 1).

As can be seen from the data presented in **Figure 14**, the sensor created on the basis of the Pt/SnO₂ nanomaterial can measure hydrogen in air in a wide range of its concentrations (from 3 to 935 ppm).

In the logarithmic scale, the dependence of the conductivity of the sensor on the concentration of hydrogen in air becomes linear (**Figure 14**, curve 2) [31, 32]. That is very convenient to use the sensor in practice, because its periodic calibration, that usually accompanies the long-term operation of the sensor, can be carried out only by two concentrations of hydrogen-air mixtures.

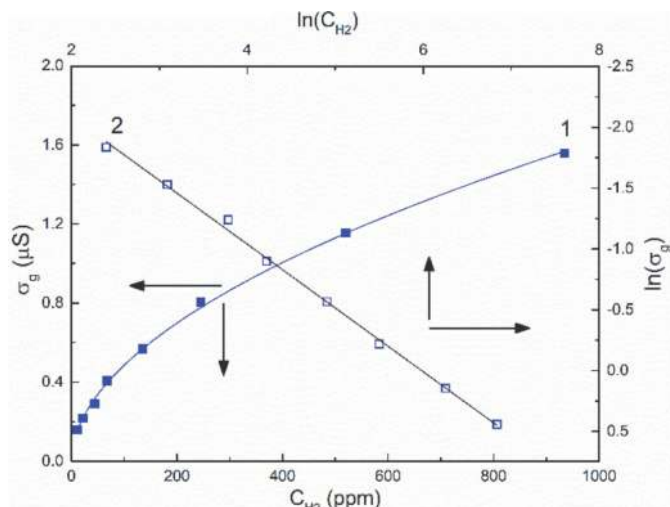


Figure 14. Dependence of electrical conductivity of the platinum-containing sensor on hydrogen concentration in air (1) and its linearized form in the logarithmic scale (2).

One of the most important properties of sensors is the reproducibility of their performance over a period of their operation. The data presented on **Figure 15** shows a change in the conductivity of the sensor with periodic supply of 44 ppm H_2 for 100 minutes of its continuous operation. As it can be seen, the sensor signal is well reproduced - a deviation of its signal value does not exceed ($\pm 4\%$) from the initial value.

Table 3 shows the data on the stability of the sensor response in the presence of 44 ppm H_2 during continuous operation for a working day (8 hours). As it can be seen, a deviation of the response value of the sensor (Δ) from its initial value (in the first hour of the sensor operation) is insignificant, that indicates to sufficient stability of the sensor.

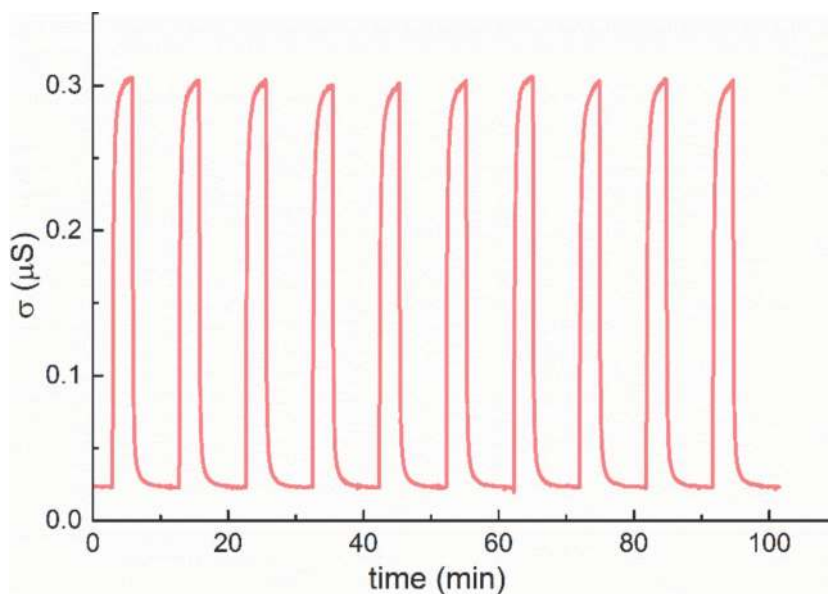


Figure 15. The reproducibility of the platinum-containing sensor signal to 44 ppm of H_2 for 100 minutes of the sensor operation at its temperature of 595 K.

Sensor response and its change	Time (hours)							
	1	2	3	4	5	6	7	8
γ	13.22	12.95	13.412	13.21	13.66	13.19	13.24	13.59
Δ (%)		-1.98	1.45	-0.05	3.38	-0.20	0.21	2.82

Table 3.
 Stability of the sensor response to 44 ppm H₂ at a sensor temperature of 595 K for 8 hours of the sensor continuous operation.

The results of measuring the sensor response to 22 ppm of hydrogen before and after overloading the sensor with hydrogen (935 ppm), are presented in **Figure 16**.

As it can be seen from the above data, the hydrogen overload has almost no effect on the value of the conductivity of the sensor, that corresponds to the presence in air of a H₂ microconcentration (22 ppm). This indicates to the stability of the material of the gas-sensitive layer, that remains unchanged when exposed to a high concentration of hydrogen at relatively high operating temperatures of the sensor. Thus, the sensor is able to correctly measure the hydrogen content even after exposure to almost 50 times the concentration of H₂. This, of course, indicates to possibility of the stable sensor operation in real conditions. In addition, these data confirm good dynamics of the sensor, because it quickly returns to its initial state in air after exposure of high hydrogen concentrations to it. In particular, it was found that at the operating temperature of 595 K, the response time of the sensor ($t_{0.9}$) in relation to 22 ppm H₂ is 10 s, and the relaxation time is 30 s.

To assess a possible effect on the conductivity of the sensor of carbon monoxide and methane, which are also classified as fire precursor gases and which appear in air of the room behind hydrogen, the same CO and H₂ concentration in air were applied to the sensor. It was found (**Figure 17**), that the conductivity of the sensor in the presence of H₂ is much higher than for CO (the value of the conductivity of the sensor for CO is about 10% of the conductivity of the sensor to H₂), and the sensor is practically not felt CH₄

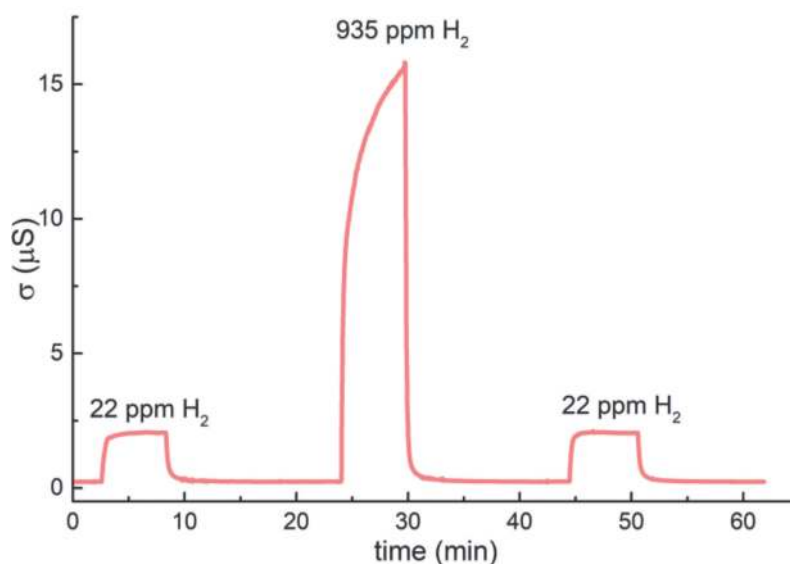


Figure 16.
 Change in the conductivity of the platinum-containing sensor to 22 ppm of hydrogen after its exposure to 935 ppm of hydrogen at a sensor temperature 595 K.

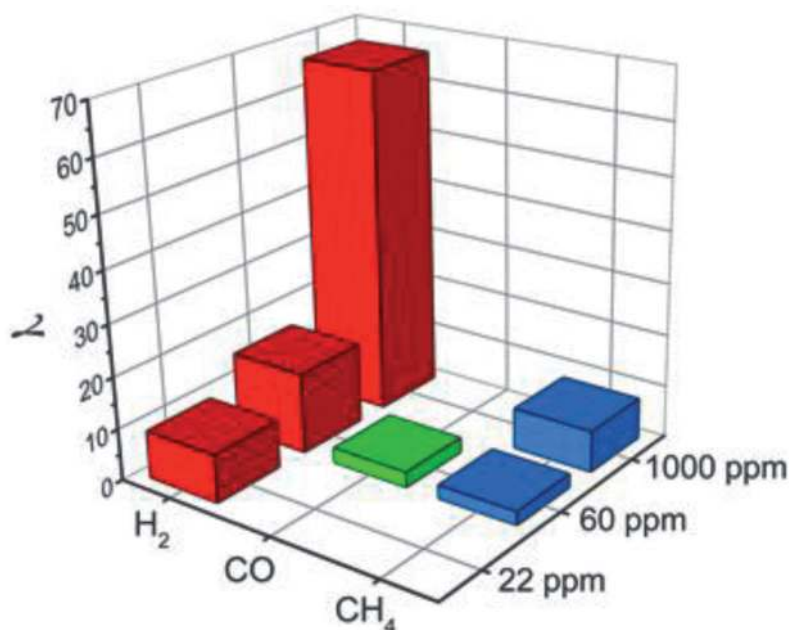


Figure 17.

The response of the Pt/SnO₂-based sensor to different concentrations of hydrogen (22 ppm), carbon monoxide (60 ppm) and methane (935 ppm).

at even much higher concentration (935 ppm) than for H₂. Since CO and CH₄ appear in air after some time after the appearance of hydrogen, and the sensor response time for H₂ is 10 seconds, it becomes clear that such sensor can detect the presence of H₂ before presence of CO and CH₄ in air and thus detect the earliest stage of appearance of the fire.

The proposed sensor for the fire diagnostics will have the following advantages in comparison with already known analogues: presence of the open flame will not be necessary for generating the alert (as in the case of the heat or smoke detectors), and the detector will not be impeded by the dust (as in the case of the optical sensors). The assumed high sensitivity of the sensor to H₂ (the first precursor of the fire) and the good response time will allow to determine the onset of smoldering at the earliest stage before the start of the open fire). In addition, taking into account the low power consumption of the sensors (0.4 watts), they can be used in controlled rooms with organizing their power supply from the electrical networks, that is usually presented in the rooms, which is convenient when using sensors in practice.

It should be noted that production of hydrogen is usually highest at first stage of the ignition while with appearance of the open fire production of hydrogen can drastically decrease [7, 33] while production of smoke and other organic and inorganic compounds (such as benzene, biphenyl, ethane, hydrogen chloride, hydrogen cyanide etc.) has begun [33]. This fact allows to suggest the use of the created hydrogen sensor with other type fire sensors in a complex device. This will allow to determine the initial stage of the fire situation by monitoring of the hydrogen sensor signal and to track fire development.

4. Conclusions

In this work by using a sol-gel method sensor material based on nanosized tin dioxide with an average particle size of 10–11 nm was created and possibility of its


use as a gas-sensitive layer of the semiconductor hydrogen sensor was investigated. It was found that the addition of platinum to the synthesized nanomaterial increases the sensitivity of sensors to hydrogen compared to tin dioxide. It was shown that due to high sensitivity to hydrogen, fast response time, a wide range of H₂ detectable concentrations in air, resistance to hydrogen overloads, good reproducibility of the sensor signal and selectivity to hydrogen measurement, the created sensor is promising for use in the detector of early warning of the fire.

Author details

Nelli Maksymovych*, Ludmila Oleksenko and George Fedorenko
Taras Shevchenko National University of Kyiv, Ukraine

*Address all correspondence to: nellymax@univ.kiev.ua

IntechOpen

© 2021 The Author(s). Licensee IntechOpen. This chapter is distributed under the terms of the Creative Commons Attribution License (<http://creativecommons.org/licenses/by/3.0>), which permits unrestricted use, distribution, and reproduction in any medium, provided the original work is properly cited. 

References

- [1] Center of Fire Statistic. World Fire Statistics [Internet]. 2020. Available from: https://www.ctif.org/sites/default/files/2020-06/CTIF_Report25.pdf [Accessed: 2021-06-02]
- [2] Sam Kubba. Impact of Energy and Atmosphere. In: Sam Kubba, editor. LEED v4 Practices, Certification, and Accreditation Handbook. 2nd ed. Oxford: Butterworth-Heinemann, Elsevier; 2016. p. 409-518. DOI: 10.1016/B978-0-12-803830-7.00009-8
- [3] A. Enis Çetin, Bart Merci, Osman Günay, Behçet Uğur TöreynSteven Verstockt. Methods and Techniques for Fire Detection. London: Academic Press, Elsevier; 2016. 91 p. DOI: 10.1016/C2014-0-01269-5
- [4] Simone Krüger, Anka Berger, Ulrich Krause. Chemical–analytical investigation of fire products in intermediate storages of recycling materials. *Fire and Materials*. 2012;36:165-175. DOI: 10.1002/fam.1098
- [5] Simone Krüger, Anja Hofmann, Anka Berger, Nicolas Gude. Investigation of smoke gases and temperatures during car fire – large-scale and small-scale tests and numerical investigations. *Fire and Materials Fire Mater*. 2016;40:785-799. DOI: 10.1002/fam.2342
- [6] Ayako Sawada, Tsubasa Higashino, Takashi Oyabu, Yoshinori Takei, Hidehito Nanto, Kiyoshi Toko. Gas sensor characteristics for smoldering fire caused by a cigarette smoke. *Sensors and Actuators B: Chemical*. 2008;130:88-93. DOI: 10.1016/j.snb.2007.07.083
- [7] Simone Krüger, Marie-Claire Despinasse, Tina Raspe, Kai Nörthemann, Werner Moritz. Early fire detection: Are hydrogen sensors able to detect pyrolysis of house hold materials? *Fire Safety Journal*. 2017;91:1059-1067. DOI: 10.1016/j.firesaf.2017.04.035
- [8] C. Wang, L. Yin, L. Zhang, D. Xiang, R. Gao. Metal Oxide Gas Sensors: Sensitivity and Influencing Factors. *Sensors*. 2010;10:2088-2106. DOI: 10.3390/s100302088
- [9] D. Kohl. Surface processes in the detection of reducing gases with SnO₂-based devices. *Sensors and Actuators*. 1989;18:71-113. DOI: 10.1016/0250-6874(89)87026-X
- [10] George Fedorenko, Ludmila Oleksenko, Nelly Maksymovych, Inna Vasylenko. Cerium-doped SnO₂ nanomaterials with enhanced gas-sensitive properties for adsorption semiconductor sensors intended to detect low H₂ concentrations. *Journal of Materials Science*. 2020;55:16612-16624. DOI: 10.1007/s10853-020-05199-w
- [11] George F. Fine, Leon M. Cavanagh, Ayo Afonja, Russell Binions. Metal Oxide Semi-Conductor Gas Sensors in Environmental Monitoring. *Sensors*. 2010;10:5469-5502. DOI: 10.3390/s100605469
- [12] A.V. Marikutsa, M.N. Rumyantseva, A.M. Gaskov, A.M. Samoylov. Nanocrystalline Tin Dioxide: Basics in Relation with Gas Sensing Phenomena. Part I. Physical and Chemical Properties and Sensor Signal Formation. *Inorganic Materials*. 2015;51:1329-1347. DOI: 10.1134/S002016851513004X
- [13] Noboru Yamazoe, Kengo Shimanoe. New perspectives of gas sensor technology. *Sensors and Actuators B: Chemical*. 2009;138:100-107. DOI: 10.1016/j.snb.2009.01.023

- [14] Nicolae Barsan, Udo Weimar. Conduction model of metal oxide gas sensors. *Journal of Electroceramics*. 2001;7:143-167. DOI: 10.1023/A:1014405811371
- [15] Ludmila Oleksenko, George Fedorenko, Nelly Maksymovych. Effect of heterogeneous catalytic methane oxidation on kinetics of conductivity response of adsorption semiconductor sensors based on Pd/SnO₂ nanomaterial. *Research on Chemical Intermediates*. 2019;45:4101-4111. DOI: 10.1007/s11164-019-03893-2
- [16] Ašperger S. Chemical Kinetics and Reaction Mechanisms. In: *Chemical Kinetics and Inorganic Reaction Mechanisms*. Boston: Springer; 2003 p.3-103. DOI: 10.1007/978-1-4419-9276-5_2
- [17] G. Korotcenkov, S.-D. Han, B.K. Cho, V. Brinzari. Grain Size Effects in Sensor Response of Nanostructured SnO₂- and In₂O₃-Based Conductometric Thin Film Gas Sensor. *Critical Reviews in Solid State and Materials Sciences*. 2009;34:1-17. DOI: 10.1080/10408430902815725
- [18] Emil Roduner. Size matters: why nanomaterials are different. *Chemical Society Reviews*. 2006;35:583-592. DOI: 10.1039/B502142C
- [19] Boris V. L'vov, Andrew K. Galwey. Catalytic oxidation of hydrogen on platinum: Thermochemical approach. *Journal of Thermal Analysis and Calorimetry*. 2013;112:815-822. DOI: 10.1007/s10973-012-2567-0
- [20] Kalim Deshmukh, Tomáš Kovářík, Tomáš Křenek, Denitsa Docheva, Theresia Stich, Josef Pola. Recent advances and future perspectives of sol-gel derived porous bioactive glasses: a review. *RSC Advances*. 2020;10:33782-33835. DOI: 10.1039/D0RA04287K
- [21] Mritunjaya Parashar, Vivek Kumar Shukla, Ranbir Singh. Metal oxides nanoparticles via sol-gel method: a review on synthesis, characterization and applications. *Journal of Materials Science: Materials in Electronics*. 2020;31:3729-3749. DOI: 10.1007/s10854-020-02994-8
- [22] C. Jeffrey Brinker, George W. Scherer. *Sol-Gel Science. The Physics and Chemistry of Sol-Gel Processing*. San Diego: Academic Press; 1990. 908 p. DOI: 10.1016/C2009-0-22386-5
- [23] E. V. Sokovykh, L. P. Oleksenko, N. P. Maksymovych, I. P. Matushko. Influence of temperature conditions of forming nanosized SnO₂-based materials on hydrogen sensor properties. *Journal of Thermal Analysis and Calorimetry*. 2015;121:1159-1165. DOI: 10.1007/s10973-015-4560-x
- [24] C. Hammond. *The basics of crystallography and diffraction*. 4th ed. Oxford: Oxford university press; 2015. 507 p. DOI: 10.1093/acprof:oso/9780198738671.001.0001
- [25] Holger Borchert, Elena V. Shevchenko, Aymeric Robert, Ivo Mekis, Andreas Kornowski, Gerhard Grübel, Horst Weller. Determination of Nanocrystal Sizes: A Comparison of TEM, SAXS, and XRD Studies of Highly Monodisperse CoPt₃ Particles. *Langmuir*. 2005;21:1931-1936. DOI: 10.1021/la0477183
- [26] I.V. Vasylenko, S.V. Kolotilov, I.E. Kotenko, K.S. Gavrilenko, F. Tuna, G.A. Timco, R.E.P. Winpenny, V.V. Pavlishchuk. Magnetic properties of nanosized γ -Fe₂O₃ and α -(Fe_{2/3}Cr_{1/3})₂O₃, prepared by thermal decomposition of heterometallic single-molecular precursor. *Journal of Magnetism and Magnetic Materials*. 2012;324:595-601. DOI: 10.1016/j.jmmm.2011.08.049

- [27] George Fedorenko, Ludmila Oleksenko, Nelly Maksymovych, Galina Skolyar, Oleksandr Ripko. Semiconductor Gas Sensors Based on Pd/SnO₂ Nanomaterials for Methane Detection in Air. *Nanoscale Research Letters*. 2017;12:329. DOI: 10.1186/s11671-017-2102-0
- [28] Maria Cristina Carotta, Michele Benetti, Elena Ferrari, Alessio Giberti, Cesare Malagù, Marco Nagliati, Beatrice Vendemiati, Giuliano Martinelli. Basic interpretation of thick film gas sensors for atmospheric application. *Sensors and Actuators B: Chemical*. 2007;126:672-677. DOI: 10.1016/j.snb.2007.04.016.
- [29] C. Malagù, V. Guidi, M. Stefancich, M. C. Carotta, G. Martinelli. Model for Schottky barrier and surface states in nanostructured n-type semiconductors. *Journal of Applied Physics*. 2002;91:808-814. DOI: 10.1063/1.1425434
- [30] A.I. Buvaylo, L.P. Oleksenko, N.P. Maksimovich, I.P. Matushko, A.P. Ripko, V.P. Ruchko. Effect of SnO₂ particle size on the hydrogen sensitivity of adsorption-semiconductor sensors with Co_xO_y/SnO₂ active coating. *Theoretical and Experimental Chemistry*. 2010;46:153-157. DOI: 10.1007/s11237-010-9132-3
- [31] S. Roy Morrison. Mechanism of semiconductor gas sensor operation. *Sensors and Actuators*. 1987;11:283-287. DOI: 10.1016/0250-6874(87)80007-0
- [32] Noboru Yamazoe, Kengo Shimano. Theory of power law for semiconductor gas sensors. *Sensors and Actuators B: Chemical*. 2008;128:566-573. DOI: 10.1016/j.snb.2007.07.036
- [33] Ministry of Housing, Communities & Local Government of United Kingdom. Grenfell environmental checks: review of combustion related fire products. [Internet]. 2020. Available from: https://assets.publishing.service.gov.uk/government/uploads/system/uploads/attachment_data/file/928024/Combustion_related_fire_products_review_ISSUE.pdf [Accessed: 2021-06-19]